
Can hammerhead ribozymes be efficient tools to inactivate gene function?

Edouard Bertrand⁺, Raymond Pictet* and Thierry Grange[§]

Institut Jacques Monod du CNRS, Université Paris 7, Tour 43, 2 Place Jussieu, 75251 Paris Cedex 05, France

Received November 5, 1993; Revised and Accepted December 20, 1993

ABSTRACT

In order to improve hammerhead ribozyme efficiency and specificity, we have analyzed, both *in vitro* and *in vivo*, the activity of a series of ribozyme/substrate combinations that have the same target sequence but differ in the length of the ribozyme/substrate duplex or in their structure, *i.e.*, the total length of the RNA. *In vitro*, we have found that optimal *k*_{cat}/*K*_m (at 37°C) is obtained when the ribozyme/substrate duplex has a length of 12 bases, which according to the base composition represents a calculated free energy of binding of –16 kcal/mol. We discuss the importance of this value for ribozyme specificity and present strategies that may improve it. Increasing the length of the duplex from 14 to 17 bases (from –19 to –26 kcal/mol) produces a reduced ribozyme activity which is probably due to a slower rate of product dissociation. In addition, inclusion of either the substrate or the ribozyme in a long transcript produces a reduction (10 fold) of the *k*_{cat}/*K*_m, probably because of a different accessibility of the target sequence. *In vivo*, the activity of the *trans*-acting ribozyme was extremely low and detected in only one case: with a ribozyme/substrate duplex length of 13 bases and with both ribozyme and substrate embedded in short RNAs expressed at a very high level. The similarity of the results obtained *in vitro* and *in vivo* indicates that it is possible to use an *in vitro* system to optimize ribozymes which are to be used *in vivo*. Satisfactory results were obtained *in vivo* only with *cis*-acting ribozymes. Altogether these results suggest that the ribozyme/substrate hybridization step is the limiting step *in vivo* and therefore it is not clear if ribozymes represent an improvement over antisense RNAs.

INTRODUCTION

Reverse genetics, *i.e.*, specific inactivation of a gene or a gene product, has become a major tool in the study of mammalian development. Reverse genetics can be directed at 3 distinct targets:

DNA, RNA, and proteins, using respectively homologous recombination (1, 2), ribozymes (3, reviewed in 4), antisense nucleic acids (5–9), and antibodies (10, 11). Antisense and ribozyme sequences can be linked to a promoter and this chimeric gene introduced in cells or animals. Depending upon the regulatory sequence selected, these molecules provide a unique possibility for the construction of a time and/or tissue-specific suppressor gene.

The importance of hammerhead ribozymes is based on their ability to irreversibly inactivate their targets and to turn-over *in vitro* (3, 12, 13). *In vivo*, these molecules appear to be able to produce a phenotype (14–24) which in few instances is associated with detectable target RNA cleavage (16, 17).

The most versatile design for *trans*-acting hammerhead complexes (3) consists of two parts: 1) a catalytic core formed by 13 conserved nucleotides and a stem loop structure (stem II); 2) two variable sequences, which together form the specifier sequence (Spc), located on each side of the catalytic core. This Spc sequence allows the enzyme to hybridize to a complementary target sequence (Ta) present in the substrate RNA. The ribozyme/substrate hybrid restores the two stems (I and III) that are part of the full hammerhead structure (25). Upon cleavage of the substrate, the products can dissociate from the ribozyme, allowing turn-over (3, 12, 13).

To specifically inactivate a target RNA *in vivo*, the ribozymes must cleave with high efficiency a single mRNA species within the complex RNA population of a eukaryotic cell. In this study, we have focused upon the specificity of hammerhead ribozymes and optimization of their activity. Specificity was evaluated by determining the minimal length of the target sequence required for substrate cleavage. Activity was analyzed *in vitro*, under conditions (such as temperature, ionic conditions, and target RNA structure) that mimics the *in vivo* situation. The parameters found to be important for efficient ribozyme activity *in vitro* (target and enzyme structure, target and enzyme levels, ribozyme-target duplex length) were then tested *in vivo*. We found low activity but a good correlation between the *in vivo* and *in vitro* results.

*To whom correspondence should be addressed

Present addresses: ⁺Beckman Research Institute of the City of Hope, Department of Molecular Genetics, 1500 E. Duarte Rd, Duarte, CA 91010 and

[§]University of California, San Francisco, Department of Biochemistry and Biophysics, CA 94143-0448, USA

MATERIALS AND METHODS

Plasmids constructions

A detailed description of plasmid constructions is available upon request. Synthetic oligonucleotides were cloned in the polylinker of the Bluescript™ family of plasmids. All constructions involving oligonucleotides and PCR were verified by DNA sequencing. The RNA sequences are given as DNA.

Ribozymes sequences

R1: **TCTAGACTTGTAAACTGATGAGTCCGTGAGGACGAAACAAGGGG-GGTACC**
 R2: **GGTACCTAGAGAACA**CTGATGAGTCCGTGAGGACGAAACTTTGATTGGATCC
 R3: **TCTAGACCCACTCTCTGATGAGTCCGTGAGGACGAAACTACTTCCTGCAG**
 R3mt: **TCTAGACCCACTCTTTGATGAGTCCGTGAGGACGGA**ACT-**ACTTCCTGCAG**
 R3s: **CTGCAGAGATCTCATAGATCACTCTCTGATGAGGCCAAAAGGCCGAAACTACTTAAAGTCGAC**
 R4: **GAGCTCCACCAATCTGATGAGTCCGTGAGGACGAAACTTTTCCAGATCT**
 R5: **AGATCTTTGATTGACTGATGAGTCCGTGAGGACGAAACTCGTTTCTGCAG**

The respective cleavage sites in Pit-1 mRNA (26) are located at positions 232 (R1), 838 (R2), 773 (R3), 346 (R4) and 826 (R5), according to the numbering of Pit-1 cDNA sequence. Their Spc sequences are underlined. The mutated positions in R3mt are indicated as bold, italic letters. Ribozymes sequences were first synthesized as DNA oligonucleotides, and cloned into Bluescript™ SK+ or KS+. The restriction sites used for cloning are indicated by bold letters. The resulting plasmids are pR1, pR2, pR3, pR3mt, pR3s, pR4, pR5. The diribozyme (pR3-R4), and the pentaribozyme (pR1-R5) were obtained by subcloning into Bluescript™ SK+. The diribozyme contains, in the order of transcription from the T7 promoter R3+R4, and the pentaribozyme contains R1+R2+R3+R4+R5.

Short substrates sequences

S17: **TCTAGATGAAGTAGTAAGAGTGTGGTCTGCAG**
 S17b: **CTGCAGAGATCTCATAAAGAAGTAGTAAGAGTGTGGTTAAGCTT**
 S14: **TCTAGATTAAGTAGTAAGAGTGTCTGCAG**
 S13: **TCTAGAGGTAGTAAGAGTTCTGCAG**
 S12: **TCTAGACCAAGTAGTAAGAGTGCCTGCAG**
 S11: **TCTAGACCAAGTAGTAAGAGTCCTGCAG**
 S10: **TCTAGACCCGTAGTAAGAGTCCTGCAG**
 S8: **TCTAGATAGTAAGAGCTGCAG**

Each substrate is named S followed by a number which corresponds to the length of the Ta sequence (underlined). Substrates were synthesized as DNA oligonucleotides and cloned in Bluescript™ KS+ (the restriction sites used are indicated by bold letters). The resulting plasmids are: pS17, pS17b, pS14, pS13, pS12, pS11, pS10 and pS8.

Pit-1 cloning. A cDNA containing the entire coding sequence of Pit-1 was amplified by PCR (27, 28, 29), from total RNA of GH3 cells, using the following oligonucleotides: GCTCTTAGATCTCTACTCTCTTGTGGGAATG, and CACATGGGTA-CCACAGGCAAGTCTTATCTGC. Plasmid pPit corresponds to the resulting cDNA cloned into Bluescript™ KS+.

RNA synthesis and *in vitro* cleavage reaction

Plasmids were linearized (pR1 and pR2 with Bam HI; pR4 and pR3-R4 with Bgl II; pR1-R5, pR3, pS17, pS14, pS12, pS13 with Pst I; pPit with Kpn I; pS8 with Eco RI), digested with Pvu II and the ends filled-in with Klenow. The resulting fragments were transcribed *in vitro* using T7 RNA polymerase as described (30), except that the reaction contained either 0.2 mM or 0.02 mM CTP, and 20 or 4 μCi of α³²P CTP respectively. For the experiment summarized in Table III, 0.2 mM UTP and 0.25 μM of α³⁵S UTP (20 μCi) were used. α³⁵S UTP has been reported to inhibit the cleavage reaction in some cases (31, 32). However, we have not observed this effect with the dilution used here (data not shown). After a 1 hour incubation at 37°C, nucleic acids were phenol-chloroform extracted and ethanol precipitated. RNA concentrations were calculated using the percentage of nucleotide incorporation in TCA insoluble material (between 25–65%). The quality of RNA was assessed on a denaturing polyacrylamide gel. For Pit-1 RNA, an additional shorter band was obtained (10% of the incorporated radioactivity), presumably due to a premature transcription termination.

Cleavage reactions were performed at 37°C in 20 mM Tris-HCl; 20 mM MgCl₂; 150 mM NaCl; pH 7.5 at 37°C. Ribozymes and substrates were heated separately for 1 min. at 90°C in water, renatured 5 min. at 37°C in the cleavage buffer, and then mixed. Reactions were stopped by addition of ice-cold EDTA (40 mM final), and analyzed on denaturing polyacrylamide (4–8%) gels. Bands were located by autoradiography, excised and counted by liquid scintillation, or alternatively the radioactivity was quantified on the gel with an AMBIS radioanalytic imaging system.

Cotransfection assays

Human hepatoma cells (HepG2, 33) were grown in DMEM supplemented with 10% fetal calf serum. Transfections were performed with the calcium phosphate coprecipitation procedure (34) using 200 ng of the substrate expressing vector, 20 μg of either the ribozyme expressing vector or the same vector but without the ribozyme sequences as a control, and 2 μg of a reference plasmid to correct for variation of transfection efficiency [pL30CAT, that expresses the CAT mRNA from the L30 promoter (35 and M.Fromont-Racine; unpublished results). For the experiments involving *cis*-acting ribozymes, 20 μg of the expression vector and 2 μg of pL30CAT were used. The precipitate was left on the cells for 20 hours and the cells were collected after 42 additional hours.

Cellular RNA analysis

Total RNA was prepared with the LiCl/Urea method, as previously described (36). Remaining DNA was removed using DNase I (RNase-free; Promega). After phenol-chloroform extraction the RNA was ethanol precipitated.

Measurements of RNA levels. RNA levels were measured by a quantitative RT-PCR assay (37), where the target RNA and CAT mRNA were simultaneously amplified in the same reaction in order to correct for variations in reverse transcription, PCR and transfection efficiencies.

The primers were positioned on each side of the target cleavage site in order to amplify only the intact substrate. The primers are:

for CAT, #1: TCACGGATATACCACCGTTGA; #2: GTTACATTG-AGCAACTGACTGA;

for S17b, #1: TCGACGGTATCGATAAGCTTAA; #2: TAAAAGAAG-TAGTAAGAGTATGG;
 for Pit-1, #1: TATCTGCACTCAAGATGCTCCTT; #2: GATCATGCG-GATGGCTGAAGAA;
 for R3s, #1: ACTTAAAGTAGTTTCGGCCTTTTG; #2: TAGATCACTC-TCTGATGAGGC.

The assay was performed as follows: 1 μ g of total RNA and 10 ng of the suitable primer # 1 were denatured at 95°C for 3 min. in 6 mM MgCl₂, 65 mM Tris-HCl, 16.5 mM (NH₄)₂SO₄, 10 mM β -mercaptoethanol, pH 8.8. The hybridization was then performed at 42°C for 30 min. The dNTP (500 μ M final) and 3 Units of AMV reverse transcriptase (Stratagene) were added and the reaction incubated at 42°C for 30 min. The enzyme was inactivated at 95°C for 5 min. before starting the PCR. This was performed in the same buffer containing 0.4 mM MnCl₂, 200 μ g/ml BSA (DNAse free), 3 mM MgCl₂, the suitable ³²P labeled primers # 2 (either 10 ng, for Pit-1 and S17b expressed from pPII and pRU₁ or 100 ng, for CAT and S17b expressed from pIU₁) and additional primers # 1 (either 10 or 100 ng). PCR products were then resolved by polyacrylamide gel electrophoresis. After autoradiography, the bands were excised and counted. The amount of PCR product amplified from the target RNA was then divided by the one amplified from CAT mRNA. We found that variations in the quantification of the RNAs were not higher than \pm 20% when the PCR was performed for less than 20 cycles (a single cycle consists of 30 sec. at 94°C, 2 min. at 59°C and 3 min. at 74°C), and when less than 5% of each oligo was elongated during the PCR (data not shown).

The absolute number of molecules of R3s per cell transfected with 20 μ g of pIU₁-R3s has been estimated as follows: Using labeled primer # 1, we have quantified the specific primer extension products obtained with total RNA of transfected cells. The amount per cell was then estimated assuming that reverse transcription efficiency was 100%, transfection efficiency 10% (data not shown), and total amount of RNA per cell 30 pg (38).

Detection of substrate cleavage. The RLPCR (Reverse Ligation PCR) procedure and the primers used for the 950 base long Pit-1 mRNA have been previously described (39). The sequence of the primers used for the analysis of S17b are: primer # 1: GT-CGACGGTATCGATA; primer # 2 is the primer # 1 used for S17b during RT-PCR.

RESULTS

In vitro analyses

As a preliminary to the *in vivo* analyses of ribozyme activity, we studied a series of parameters *in vitro*, using conditions of ionic strength, pH and temperature that mimics the *in vivo* situation.

Length of the enzyme/substrate hybridizing region. The overall ribozyme efficiency is likely to depend on both the length and base composition of the Spc sequence that hybridizes with the Ta sequence in the substrate. Optimal efficiency will be provided with any Ta/Spc sequence long enough to allow formation of a sufficiently stable enzyme/substrate complex, but short enough to allow a high rate of product release. On the other hand, the shortest Ta that provides efficient cleavage defines the ribozyme specificity, because, theoretically, the ribozyme will efficiently cleave any RNA that shares this minimal Ta sequence.

To estimate the importance of these two parameters, we carried single and multiple turn-over kinetic analyses of different enzyme/substrate combinations (Fig. 1 and Table I). This analysis was performed using the R3 enzyme with several substrates approximately 60 nucleotide long (S8, S10, S11, S12, S13, S14 and S17) that differ by the length of the Ta which is respectively 8 (38% GC), 10 (40% GC), 11 (36% GC), 12 (42% GC), 13 (46% GC, but has one GU base-pair with R3), 14 (36% GC) or 17 (47% GC) bases. The Ta sequence occupies both sides of the cleavage site with the following distributions: 4+4 (S8), 5+5 (S10), 6+5 (S11), 6+6 (S12), 8+5 (S13), 7+7 (S14) and 9+8 bases (S17). Single turn-over kinetics shows that S8, S10 and S11 were cleaved very poorly, even with a large excess of enzyme over substrate (Table I). Substrates S12, S13, S14 and S17 have similar kcat/Km (Fig. 1 and Table I), setting the minimal Ta length for the activity of this ribozyme at 12 bases.

Under multiple turn-over conditions, substrates S12, S13 and S14 have similar cleavage velocity. In contrast, S17 is 3–4 times slower (Table II). All these substrates have similar kcat/Km values, under single turn-over conditions. Therefore, this difference is probably due to a slower release of the cleavage products when the Ta is increased from 14 to 17 bases.

Influence of enzyme and substrate structure on ribozyme efficiency. Most RNAs form complex secondary and tertiary structures (41). In general, the shorter is the RNA, the lower is the probability to adopt stable structures. Therefore, short RNA targets should be better substrates for ribozymes than longer ones. To test this hypothesis, we compared the kinetics of the R3

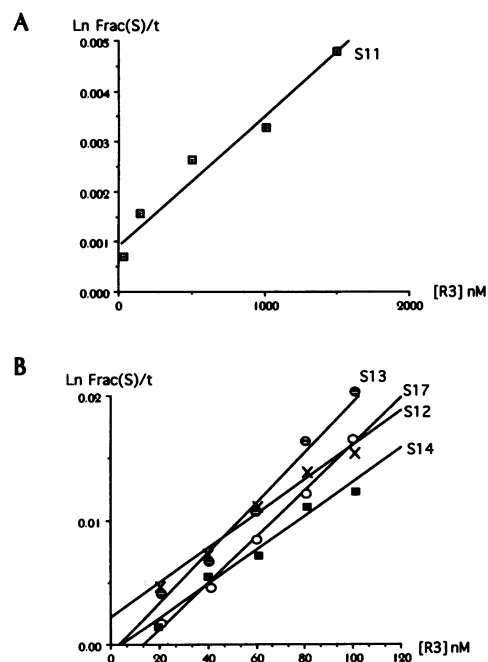


Figure 1. Effect of the size of the Ta region on single turn-over kinetics. A constant concentration of substrate (2 nM) is incubated with increasing concentration of ribozyme (50, 150, 500, 1000 and 1500 nM in A, and 10, 20, 40, 60, 80 and 100 nM in B) for 30 min. at 37°C. (Ln Frac (S))/t is then plotted against the ribozyme concentration, where Frac (S) is the fraction of remaining substrate. The curves are then fitted to a line, which slope is kcat/Km (46). A. Substrate S11. B. Substrates S12, S13, S14 and S17.

Table I. Single turn-over kinetics: effect of the length of Ta

R3/Substrate couples	R3/S8	R3/S10	R3/S11	R3/S12	R3/S13	R3/S14	R3/S17
kat/Km* 10 ⁻⁶ nM ⁻¹ min ⁻¹	<1	<1	2,6	170	211	250	100
ΔG ^o [§] kcal/mol	-8,2	-12,6	-14,3	-16,1	-16,9	-19,1	-26,1

*The kat/Km are averaged from two to three determinations using a substrate concentration of 2 nM and a concentration of ribozyme varying between 10 and 100 nM for S12, S13, S14 and S17 and between 50 and 1500 nM for S8, S10 and S11.

§The ΔG^o are estimated at 37°C as described (55). The hammerhead core was assimilated to a single phosphodiester bond.

Table II. Multiple turn-over kinetics: effect of the length of Ta

R3/Substrate couples	R3/S12	R3/S13	R3/S14	R3/S17
k3* min ⁻¹	0.06 +/- 0.005	0.08 +/- 0.012	0.07 +/- 0.02	0.015 +/- 0.005

*Multiple turn-over kinetics were determined under steady-state conditions, at a ribozyme concentration of 100nM and at a substrate concentration of 3μM. The cleavage velocity obtained was normalized to the ribozyme concentration to give k3. The standard deviation is calculated from 3 determinations.

Table III. Single turn-over kinetics: effect of RNA structure

Enzyme/substrate couple	R1/Pit1-950	R2/Pit1-950	R4/Pit1-950	R3/Pit1-950	R3/S17
kat/Km* 10 ⁻¹ nM ⁻¹ min ⁻¹	7,3	30	7,1	20	100

*The kat/km were obtained as described in legend of figure 1 using a substrate concentration of 20 nM and ribozyme concentration between 100 and 300 nM.

ribozyme with two fragments of Pit-1 mRNA (26), of which one is 950 nucleotides long (Pit-950), and the other is 60 nucleotides long (S17). These fragments contain the same 17 nucleotides Ta sequence. Under single turn-over conditions, Pit-950 has a kat/Km 5 fold lower than S17 (Table III). This result indicates that the structure of the long substrate can limit ribozyme efficiency, presumably by hindering the hybridization step. To assess the generality of this effect, we targeted several ribozymes (R1, R2 and R4) to different regions of Pit-950 (Fig. 2A). Single turn-over kinetics performed with Pit-950 showed that these ribozymes also have a low kat/Km (Table III). These values are 3 to 15 fold lower compared to the one obtained with the R3/S17 combination (Table III). Since there is no evidence that the rate of cleavage (k₂) is affected by the base composition of the enzyme/substrate hybridizing region (42, 43), the similar inefficiency of the various ribozymes suggests that most regions of the Pit-950 molecule adopt inhibitory higher order structures.

Although *in vitro* analyses might indicate the most suitable sequences to be targeted by the ribozyme, these sequences might not be similarly accessible *in vivo* (24). Therefore, it could be useful to simultaneously target different regions of the substrate. This could be achieved in a single step by expressing a polyribozyme that contains several tandemly arranged hammerhead motifs. It has been previously shown that such polyribozymes can be active *in vitro* and *in vivo*, but the activity of the polyribozymes was not compared to the activity of a mixture of the corresponding monoribozymes (68). We have constructed two of these polyribozymes, targeted against the Pit-950 RNA: a diribozyme, that contains R3 and R4, and a pentaribozyme, that contains R1, R2, R3, R4 and R5 (Fig. 2A). Even though the polyribozymes were active, they were less efficient than the mixture of monoribozymes (Fig. 2B). Moreover, the activity of a given hammerhead motif in a polyribozyme is lower (from 2 to 10 fold) than in the mix of the single ribozymes (Fig. 2B, compare lane 4 to lane 5, and

lane 6 to lane 7), and the cleavage activity of the pentaribozyme is lower than that of R3 alone, even though R3 is present in the pentaribozyme (Fig. 2B, compare lane 2 to lane 6). These results suggest that the structure of the ribozyme moiety is also a limiting factor for the reaction efficiency.

***In vivo* activity of hammerhead ribozyme**

We have used a transient expression assay to analyze the *in vivo* activity of ribozymes using the information gained from the *in vitro* analyses. We have tested two enzymes (R3 and R3s) targeted against the same sequence, but differing in the length of the Spc sequence (17 and 13 bases respectively) and in the primary sequence of their stem II (the type of modification introduced does not affect the cleavage reaction *in vitro*, 70). Their activity was tested against two substrates of different length, but containing the same Ta sequence: the 950 base long Pit-1 mRNA (Pit-950) and a 20 base long fragment (S17b). These ribozymes and substrates were expressed using different vectors selected to satisfy the conditions derived from the *in vitro* observations (this study and 17, 21, 43–46): 1) high level of transcription and optimal stability of RNAs, 2) minimal number of potentially inactive enzyme conformations, 3) accessibility of the target. These conditions were achieved by either transcribing an enzyme surrounded by a minimal length of flanking sequences, or inserting the ribozyme into an RNA region devoid of stable secondary/tertiary structures. In order to obtain high RNA levels, we have constructed expression vectors containing the human U₁ gene (47). The vector pRU₁ allows replacement of U₁ RNA sequence by the sequence of interest such as only 10 bases of U₁ RNA 3' end remains. The other vector, pIU₁ allows insertion of a chosen sequence in place of the first 12 bases of U₁ RNA, in a region without a stable secondary/tertiary structure (48). We have also used an expression vector (pPII) which employs the strong promoter of the gene coding for the largest subunit of the RNA polymerase II (49; Fromont-Racine,

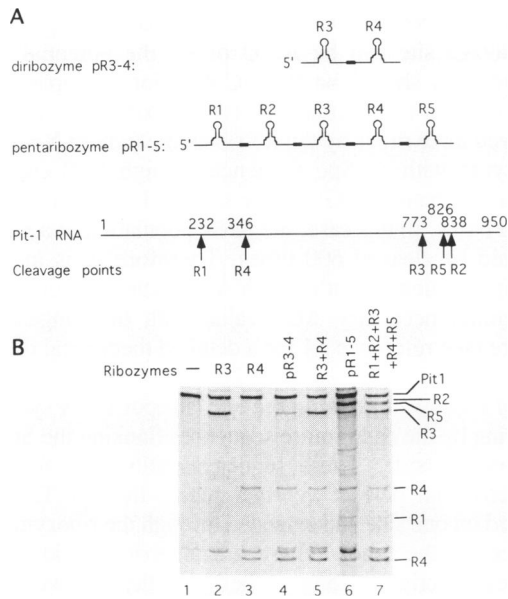


Figure 2. Effect of ribozyme structure on cleavage efficiency *in vitro*. **A.** Schematic representation of the polyribozymes pR3-4 and pR1-5. The location of the cleavage sites of each ribozyme on the synthetic Pit-1 mRNA is also indicated (the bases are numbered according to reference 26). **B.** Polyribozyme cleavage of Pit-1 mRNA. Labeled Pit-1 RNA was incubated with the ribozymes indicated on the top of the figure. The mixture of ribozymes is indicated by the sum of each ribozyme. Reactions were performed for 1 hour at 37°C, with a substrate concentration of 25 nM and a 10 fold molar excess of each enzyme over substrate. The products resulting from a single cleavage event are indicated on the right hand side by the name of the corresponding ribozyme (Pit-1 indicates the intact RNA).

R.P. and T.G., manuscript in preparation) and the polyadenylation signal originating from the HSV tk gene (50). In the resulting transcript, the sequences inserted in this vector are flanked by roughly 100 bases on both sides (excluding the poly(A) tail). We have not attempted to reduce the size of these flanking sequences because there is a risk of readthrough of the polyadenylation signal when it is too close to the promoter (51–53).

The relative efficiency of these different expression vectors was estimated by measuring the relative amount of stable R3s synthesized using a quantitative RT-PCR assay (see Material and Methods). This study reveals that pIU₁ is the most efficient vector, allowing the production of 5 fold more stable RNA than pRU₁ and 7 fold more than pPII (data not shown). The absolute number of R3s molecules present in the cells transfected with pIU₁-R3s have been estimated to be 30,000 using a quantitative reverse transcription assay (see the Materials and Methods).

We have tested various combinations of enzyme and substrate, using a constant 100 fold excess of ribozyme to substrate expression vector. Ribozyme activity was first monitored by comparing the substrate level in presence and absence of ribozyme, using a quantitative RT-PCR assay (see Material and Methods). In all the conditions tested, the ribozyme activity is not sufficient to significantly reduce the substrate level *in vivo* (Fig. 3A). We then analyzed the substrate cleavage products using the highly sensitive RLPCR procedure (39). In the experimental conditions used for the RLPCR, the PCR amplification is not quantitative and, in the absence of specific cleavage products,

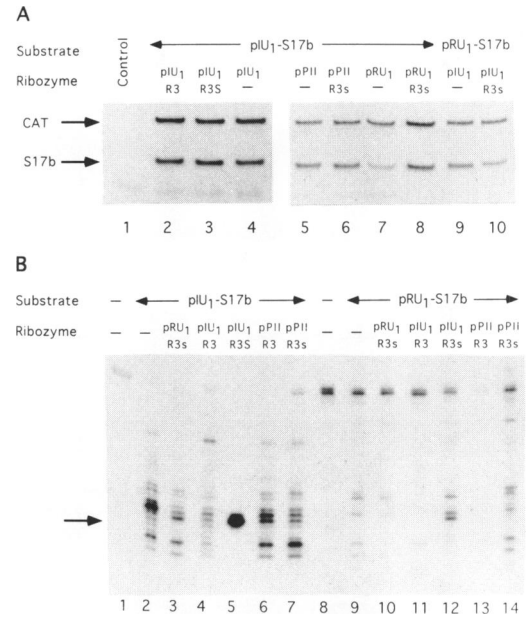


Figure 3. *In vivo* activity of *trans*-acting ribozymes. **A.** Quantification of substrate RNA using RT-PCR. The PCR products specific for S17b and CAT RNA are indicated on the left hand side of the figure. Transfections were performed with the substrate and ribozyme expression vectors shown on the top of the figure. The control expression vectors are indicated by a bar in place of the name of the ribozyme. Lane 1 is identical to lane 2 except that no reverse transcriptase was added during RT-PCR. **B.** Detection of cleavage products using RLPCR. The arrow indicates the product resulting from the ribozyme mediated cleavage. Transfections were performed with the substrate and ribozyme expression vectors shown on top of the figure. The bars indicate that no expression vectors have been used. RLPCR with the labeled primer #2 was performed for either 25 (lanes 1–7) or 30 cycles (lanes 8–14) to compensate for the different efficiencies of the expression vectors.

background degradation products are amplified (Fig. 3B, lane 2). No ribozyme specific cleavage products are seen with the long substrate (data not shown). However, a cleavage product of the expected size is observed with the small substrate, but only when the ribozyme R3s and the small substrate are expressed from the pIU₁ vector (Fig. 3B, lane 5). Since the pIU₁ is the most efficient expression vector, this result indicates that the level of both the enzyme and the substrate is a limiting factor. In addition, we showed that a ribozyme with a 13 base long Spc sequence (R3s) cleaves the substrate while the same ribozyme with a 17 base long Spc is not active (Fig. 3B, compare lane 4 and 5).

Impairments in the hybridization step could be one of the factors determining the low activity of the ribozyme *in vivo*. To test this hypothesis, we inserted the R3 and R3s ribozymes in the 3' untranslated region of the Pit-950 substrate (150 bases away from the targeted cleavage site), providing the conditions for an intramolecular reaction. In this case, the hybridization step should not be influenced by the concentration or the localization of the ribozyme. As a control, an inactivated mutant form of the ribozyme (R3mt) was also tested (see the sequence in Material and Methods). The level of Pit-950 RNA remained unchanged when linked to the mutant ribozyme (Fig. 4A). However, upon linkage of R3 and R3s to Pit-950, the ribozyme cleavage product was detected (Fig. 4B) and the level of Pit-950 RNA was lowered two fold (Fig. 4A). Thus, when acting in *cis*, R3 and R3s cleave the Pit-950 RNA.

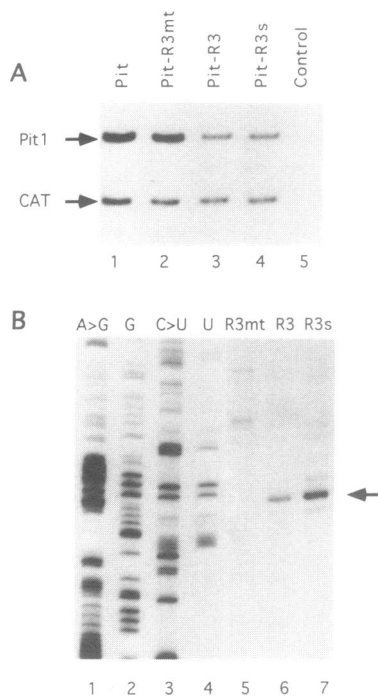


Figure 4. *In vivo* activity of *cis*-acting ribozymes. **A.** Quantification of substrate RNA in transfected cells using RT-PCR. The PCR products specific for Pit-1 and CAT RNA are indicated on the right hand side of the figure. Transfections were performed with the following expression vectors: lane 1: pPII-Pit; lane 2: pPII-Pit-R3mt; lane 3: pPII-Pit-R3; lanes 4 and 5: pPII-Pit-R3s. Lane 5 is a control identical to lane 4 except that no reverse transcriptase was added during RT-PCR. **B.** Detection of cleavage products using RLPCR. The size of the ribozyme cleavage product is indicated with an arrow. Lanes 1 to 4: Total RNA from Pit-1 expressing cells chemically cleaved at base specific location (65). Lanes 5 to 7: Total RNA from cells transfected with pPII-Pit-R3mt (lane 5), pPII-Pit-R3 (lane 6), pPII-Pit-R3s (lane 7).

DISCUSSION

Factors affecting specificity

Length of the Spc-Ta hybrid on specificity. Activity of hammerhead ribozymes depends on the stability of the hybrid formed between the specifier and its target. The lowest value of the corresponding binding free energy that still supports optimal activity was experimentally determined using the R3 ribozyme and a series of substrates. These experiments show that the R3 ribozyme still efficiently cleaves a short substrate that has a Ta length as short as 12 nucleotides (Table I). The calculated binding free energy of the Spc-Ta hybrid, which may be lower than the actual binding free energy of the corresponding ribozyme-substrate complex (42), is -16 kcal/mol. This is the lowest value for optimal activity at 37°C since the $k_{\text{cat}}/K_{\text{m}}$ of the R3/S11 combination is almost two orders of magnitude lower with a ΔG° of -14 kcal/mol.

This value can be used to estimate the specificity of hammerhead ribozymes (54). Indeed, at 37°C , a given ribozyme should cleave with an optimal $k_{\text{cat}}/K_{\text{m}}$ any RNA that is perfectly base-paired with a free energy of binding lower than -16 kcal/mol. Thus specificity will be dependent on the shortest Spc-Ta hybrid length that provides a ΔG° lower than -16 kcal/mol. This length will be referred to as N . The number of times that the Ta sequence should be present in an RNA

population of complexity C is $C/4^N$. Since the unpaired base at the cleavage site can be A, U or C, the potential ribozyme cleavage sites should be $0.75 C/4^N$. For example, the RNA population of a mammalian cell (complexity 5×10^7 bases) might be cleaved three times by the R3 ribozyme (where $N=12$). Using a ribozyme with an Spc sequence of high G/C content, it is possible to obtain a ΔG° lower than -15 kcal/mol with only 8 paired bases. In this case, the RNA population of a mammalian cell could be cleaved 600 times. Therefore, it is important to select Spc sequences with a high A/U content, in order to reach the minimal necessary ΔG° value with the longest possible sequence (see reference 54 for a detailed theoretical discussion).

Effect of sequences flanking the Spc. Proper RNA synthesis and processing by the cell require sequences flanking the Spc on both its 5' and 3' side. These sequences allow the formation of asymmetric but perfect hybrids, where the Spc-Ta pairing is shortened on one side and extended through the ribozyme flanking sequence on the other. These asymmetric hybrids should be catalytically active as long as their stability is lower than -16 kcal/mol, causing the ribozyme to cleave unwanted target sites with an optimal $k_{\text{cat}}/K_{\text{m}}$. Therefore, ribozyme flanking sequences can decrease its specificity. This effect could be greatly diminished by adding A or U residues at the 5' and 3' side of the minimal Spc sequence because they will provide the least stable base-pair. Thus all the asymmetric pairing will require a significantly longer duplex length for ribozyme activity than the symmetric one, minimizing the effect of flanking sequences on ribozyme specificity. A should be preferred to U because they avoid G-U base pairs.

Effect of mismatch on specificity; G-U base pair. The S13/R3 combination contains one G-U base pair but the corresponding $k_{\text{cat}}/K_{\text{m}}$ is similar to that of S12/R3 and S14/R3, showing that G-U base pairs do not impair ribozyme activity. This has some consequences on the ribozyme specificity as G-U pairs increase the number of sequences potentially able to form hybrids with the Spc (54). Even if the ribozyme tolerates only one G-U base pair, the number of ribozyme cleavage site per RNA population will be multiplied by the number of G plus U in the Spc sequence. The resulting decrease of specificity can be minimized by selecting a target defining an Spc sequence rich in A and C.

The effect of mismatches is difficult to predict, because they will variously affect the hybrid stability, depending on the type of mismatch and the sequence context (55). If one consider the favorable case where the ribozyme contains a minimal Spc and is flanked by A residues, this effect should not be important. Indeed, a one nucleotide bulge cost 3,3 kcal/mol and needs 4 A-U base pairs to be compensated. Thus, the number of additional sequences optimally cleaved by the ribozyme will be $3 N/4^4$, which can be neglected because N will be lower than 20 in most cases.

In conclusion, ribozymes should show non specific effects if their Spc has a high GC content or if they are flanked by GC rich sequences. Specificity can be improved by selecting a Spc rich in A and C, by using the shortest Spc that provides a hybrid stability ≤ -16 kcal/mol, and by flanking this Spc with A residues.

Factors that affect ribozyme efficiency

Structure of the ribozyme. The length of the enzyme-substrate duplex affects both enzyme-substrate hybridization and cleavage

product dissociation. By using the same enzyme on several substrates differing in their Ta length, we show that increasing the length from 14 to 17 bases decreases the ribozyme efficiency both *in vitro* and *in vivo*. *In vitro*, this increase leads to a four-fold decrease of ribozyme turn-over. Since these substrates have similar k_{cat}/K_m values under single turn-over conditions, we believe that the length increase impairs significantly the release of the cleavage products from the ribozyme. *In vivo*, this length increase leads to the disappearance of detectable cleavage products. The large excess of ribozyme over substrate achieved *in vivo* (≥ 100 -fold) suggests that the ribozyme molecules effectively active are not in excess, either because they are not localized in the same compartment as their target (15) or more generally because they do not adopt the suitable conformation. This might be related to the inhibitory effect of unfavorable ribozyme structures that we have observed *in vitro* for ribozymes embedded in polyribozymes. These observations emphasize the importance of the choice of the expression vector for the production of high levels of enzyme with minimal structures. Vectors using *cis*-acting ribozymes to trim the 5' and 3' end of the *trans*-acting ribozymes (69), or those derived from genes coding for small RNAs should be suitable for this purpose (see also 15, 56). Among the various vectors that we have constructed and tested, the one which allows insertion of the ribozymes in the unstructured 5' transcribed region of U1 gene appears to be the most efficient with high level of stable transcript and detectable ribozyme activity.

Structure of the substrate. The comparison *in vitro* between the cleavage kinetics of two substrate RNAs, differing in their length (60 vs 950 bases) but containing the same target sequence reveals that the cleavage of the longer mRNA is less efficient: it has a 5 fold lower k_{cat}/K_m under single turn-over conditions. Moreover, ribozymes targeted against different region of the mRNA have similarly low k_{cat}/K_m . Since the probability of intramolecular hybridization increases with RNA length, this difference is most likely related to an increased number of secondary or tertiary structures having a Ta sequence inaccessible to ribozyme hybridization. Indeed, several studies have shown that some substrate structures may adversely affect ribozyme efficiency (43, 46, 57).

In vivo results well correlate with the *in vitro* ones. The ribozyme activity is detected *in vivo* only with the short ribozymes and substrates, and with the expression vector that provides the highest RNA level. However the long substrate can also be cleaved if the ribozyme is located in *cis*, when the rate of association does not depend on the ribozyme concentration. Altogether, these data suggest that ribozyme/target hybridization is the crucial step *in vivo*. Therefore, the most accessible cleavage sites, *i.e.*, those devoid of extensive secondary/tertiary structure or stable protein interaction, need to be identified. *In vivo* structure probing using either enzymes or chemicals should be particularly useful for this purpose (39, 58).

Antisense RNA versus ribozyme

The concentration of enzyme required to reduce significantly the *in vivo* level of our long substrate should theoretically be 50 nM (44), which corresponds to 120,000 molecules in a 4 picoliter/cell. This represents the amount of a rather abundant cellular RNA, and might explain the low ribozyme activity we have observed *in vivo*. Although more efficient *trans*-acting ribozymes have been previously described (14–24), the cleavage

products were detected in only two cases (16, 17) and simple antisense molecules provided an effect of similar magnitude (16, 17, 19, 21–23, 45, 59). Furthermore, very high intracellular concentrations (10 to 1000 fold more than the highest concentration obtained here: 17, 21, 24) and high excess of ribozyme over substrate (from 100 to 1000 fold: 14, 16, 20, 24, 45) were necessary. In addition, it is also possible that some proteins enhancing the efficiency of ribozymes may exist in plant cells (16) or in mammalian cells upon retroviral infection. Indeed, the nucleocapsid proteins of retroviruses have both unwinding and annealing activities (60, 61) and are known to interact with the viral RNA *in vivo* (62, 63, 64). The high intracellular concentration of these proteins reached during the infection process might promote both ribozyme/substrate hybridization (annealing activity) and ribozyme turn-over (unwinding activity), as observed *in vitro* (40, E.B. and J.Rossi, manuscript in preparation), and could explain the effect described (18, 22, 23). Therefore, it is not clear if ribozyme efficiency is high enough to allow reverse genetic studies in mammals using reasonable levels of expression. Most notably, as the ribozyme/substrate binding seems to be the crucial step *in vivo*, ribozyme should not be dramatically more efficient than antisense RNAs, even though they could contribute to the improvement of the efficiency of these molecules (66). Strategies devised to colocalize the ribozyme with the target RNA within the cell might allow further significant efficiency enhancement (67).

ACKNOWLEDGEMENTS

We thank D.Castanotto, J.Deshler, J.Rossi and J.Termini for critical readings of the manuscript and helpful discussions. This work was supported by the ARC and the CNRS.

REFERENCES

- Mansour, S. L., Thomas, K. R. and Capecchi, M. R. (1988) *Nature* **336**, 348–352.
- Zimmer, A. and Gruss, P. (1989) *Nature* **338**, 150–153.
- Haseloff, J. and Gerlach, W. L. (1988) *Nature* **334**, 585–591.
- Castanotto, D., Rossi, J. J. and Deshler, J. O. (1992) *Critical Review in Eucaryotic Gene Expression* **2**, (4), 331–367.
- Izant, J. G. and Weintraub, H. (1984) *Cell* **36**, 1007–1015.
- Stephenson, M. L. and Zamecnik, P. C. (1978) *Proc. Natl. Acad. Sci. USA* **75**, 285–288.
- Zamecnik, P. C. and Stephenson, M. L. (1978) *Proc. Natl. Acad. Sci. USA* **75**, 280–284.
- Helene, C., Montenay-Garestier, T., Saison, T., Takasugi, M., Toulme, J. J., Asseline, U., Lancelot, G., Maurizot, J. C., Toulme, F. and Thuong, N. T. (1985) *Biochimie* **67**, 777–783.
- Gagnor, C., Bertrand, J. R., Thenet, S., Lemaitre, M., Morvan, F., Rayner, B., Malvy, C., Lebleu, B., Imbach, J. L. and Paoletti, C. (1987) *Nucl. Acids Res.* **15**, 10419–10436.
- Rungger-Brandle, E., Chaponnier, C. and Gabbiani, G. (1979) *Nature* **282**, 320–321.
- Wright, C. V. E., Cho, K. W. Y., Hardwicke, J., Collins, R. H. and De Robertis, E. M. (1989) *Cell* **59**, 81–93.
- Uhlenbeck, O. C. (1987) *Nature* **328**, 596–600.
- Jeffries, A. C. and Symons, R. H. (1989) *Nucl. Acids Res.* **14**, 1371–1377.
- Cameron, F. H. and Jennings, P. A. (1989) *Proc. Natl. Acad. Sci. USA* **86**, 9139–9143.
- Cotten, M. and Birnstiel, M. L. (1989) *EMBO J.* **8**, 3861–3866.
- Steinecke, P., Hergert, T. and Schreier, P. H. (1992) *EMBO J.* **11**, 1525–1530.
- Saxena, S. K. and Ackerman, E. J. (1990) *J. Biol. Chem.* **265**, 17106–17109.
- Sarver, N., Cantin, E. M., Chang, P. S., Zaia, J. A., Ladne, P. A., Stephens, D. A. and Rossi, J. J. (1990) *Science* **247**, 1222–1225.

19. Scanlon, K. J., Jiao, L., Funato, T., Wang, W., Tone, T., Rossi, J. J. and Kashani-Sabet, M. (1991) *Proc. Natl. Acad. Sci. USA* **88**, 10591–10595.
20. Sioud, M. and Drlaca, K. (1991) *Proc. Natl. Acad. Sci. USA* **88**, 7303–7307.
21. Sioud, M., Natvig, J. and Forre, O. (1992) *J. Mol. Biol.* **223**, 831–835.
22. Weerasinghe, M., Liem, S. E., Asad, S., Read, S. E. and Joshi, S. (1991) *J. Virol.* **65**, 5531–5534.
23. Dropulic, B., Lin, N. H., Martin, M. A. and Kuan-Teh, J. (1992) *J. Virol.* **66**, 1432–1441.
24. L'Huillier, P. J., Davis, S. R. and Bellamy, A. R. (1992) *EMBO J.* **11**, 4411–4418.
25. Forster, A. C. and Symons, R. H. (1987) *Cell* **49**, 211–220.
26. Ingraham, H. A., Chen, R., Mangalam, H. J., Elshltz, H. P., Flynn, S. E., Lin, C. R., Simmons, D. M., Swanson, L. and Rosenfeld, M. G. (1988) *Cell* **55**, 519–529.
27. Saiki, R. K., Scharf, S., Faloona, F., Mullis, K. B., Horn, G. T., Erlich, H. A. and Arnheim, N. (1985) *Science* **230**, 1350–1354.
28. Saiki, R. K., Gelfand, D. H., Stoffel, S., Scharf, S. J., Higuchi, R., Horn, G. T., Mullis, K. B. and Erlich, H. A. (1988) *Science* **239**, 487–491.
29. Goblet, C., Prost, E. and Whalen, R. G. (1989) *Nucl. Acids Res.* **17**, 2144.
30. Milligan, J. F., Groebe, D. R., Witherell, G. W. and Uhlenbeck, O. C. (1987) *Nucl. Acids Res.* **15**, 8783–8798.
31. Buzayan, J. M., Feldstein, P. A., Segrelles, C. and Bruening, G. (1988) *Nucl. Acids Res.* **16**, 4009–4023.
32. Buzayan, J. M., van Tol, H., Feldstein, P. A. and Bruening, G. (1990) *Nucl. Acids Res.* **18**, 4447–4451.
33. Knowles, B. B., Howe, C. C. and Aden, D. P. (1980) *Science* **209**, 497–499.
34. Graham, F. L. and Van der Eb, A. J. (1973) *Virology* **52**, 456.
35. Wiedemann, L. M. and Perry, R. P. (1984) *Mol. Cell. Biol.* **4**, 2518–2528.
36. Auffray, C. and Rougeon, R. (1980) *Eur. J. Biochem.* **107**, 303–314.
37. Wang, A. and Mark, D. F. (1990) in *PCR protocols: a guide to methods and application*, eds. Innis, M., Gelfand, D., Sninsky, J. J. & White, T. J. (Academic Press, Inc, San Diego).
38. Brandhorst, B. P. and McConkey, E. H. (1974) *J. Mol. Biol.* **85**, 451–463.
39. Bertrand, E., Fromont-Racine, M., Pictet, R. and Grange, T. (1993) *Proc. Natl. Acad. Sci. USA* **90**, 3496–3500.
40. Tsuchihashi, Z., Khosla, M., Herschlag, D. (1993) *Science* **262**, 99–102.
41. Pleij, C. W. (1990) *TIBS* **15**, 143–147.
42. Fedor, M. J. and Uhlenbeck, O. C. (1992) *Biochemistry* **31**, 12042–12054.
43. Fedor, M. J. and Uhlenbeck, O. C. (1990) *Proc. Natl. Acad. Sci. USA* **87**, 1668–1672.
44. Bertrand, E., Grange, T. and Pictet, R. (1992) in *Gene regulation: biology of antisense RNA and DNA*, eds. Erickson, R. P. & Izant, J. G. (Raven Press, New York), pp. 71–81.
45. Cotten, M., Schaffner, G. and Birnstiel, M. L. (1989) *Mol. Cell. Biol.* **9**, 4479–4487.
46. Heidenreich, O. and Eckstein, F. (1992) *J. Biol. Chem.* **267**, 1904–1909.
47. Hernandez, N. (1985) *EMBO J.* **4**, 1827–1837.
48. Parry, H. D., Scherly, D. and Mattaj, I. W. (1989) *TIBS* **14**, 15–19.
49. Ahearn, J. M., Bartolomi, M. S., West, M. L., Lisek, L. J. and Corden, J. L. (1987) *J. Biol. Chem.* **262**, 10695–10705.
50. Prost, E. and Moore, D. D. (1986) *Gene* **45**, 107–111.
51. Sanfaçon, H. and Hohn, T. (1990) *Nature* **346**, 81–84.
52. Proudfoot, N. (1991) *Cell* **64**, 671–674.
53. Iwasaki, K. and Temin, H. M. (1990) *Genes & Dev.* **4**, 2299–2307.
54. Herschlag, D. (1991) *Proc. Natl. Acad. Sci. USA* **88**, 6921–6925.
55. Freier, S. M., Kierzek, R., Jaeger, J. A., Sugimoto, N., Caruthers, M. H., Neilson, T. and Turner, D. H. (1986) *Proc. Natl. Acad. Sci. USA* **83**, 9373–9377.
56. Izant, J. G. (1992) in *Gene regulation: biology of antisense RNA and DNA*, eds. Erickson, R. P. & Izant, J. G. (Raven Press, New York), pp. 183–195.
57. King, Z. and Whitton, J. L. (1992) *J. Virol.* **66**, 1361–1369.
58. Calvet, J. P. and Myers, J. A. (1987) *J. Mol. Biol.* **197**, 543–553.
59. Joshi, S., Brunschot, A. V., Asad, S., Van Der Elst, I., Read, S. E. and Bernstein, A. (1991) *J. Virol.* **65**, 5524–5530.
60. Prats, A. C., Sarih, L., Gabus, C., Litvak, S., Keith, G. and Darlix, J. L. (1988) *EMBO J.* **7**, 1777–1783.
61. Khan, R. and Giedroc, D. P. (1992) *J. Biol. Chem.* **267**, 6689–6695.
62. Aldovini, A. and Young, R. A. (1990) *J. Virol.* **64**, 1920–1926.
63. Gorelick, R. J., Nigida, S. M., Bess, J. W., Arthur, L. O., Henderson, L. E. and Rein, A. (1990) *J. Virol.* **64**, 3207–3211.
64. Darlix, J. L., Gabus, C., Nugeyre, M. T., Clavel, F., and Barre-sinoussi, F. (1990) *J. Mol. Biol.* **216**, 689–699.
65. Peattie, D. A. (1979) *Proc. Natl. Acad. Sci. USA* **76**, 1760–1764.
66. Homann, M., Tzortzakaki, S., Rittner, K., Sczakiel, G., and Tabler, M. (1993) *Nucleic Acids Res.* **21**, 2809–2814.
67. Sullenger, B. A. and Cech, T. R. (1993) *Science* **262**, 1566–1569.
68. Chen, C. J., Banerjee, A. C., Harmison, G. G., Haglund, K., and Schubert, M. (1992) *Nucleic Acids Res.* **20**, 4581–4589.
69. Taira, K., Nakagawa, K., Nishikawa, S., and Furukawa, K. (1991) *Nucleic Acids Res.* **19**, 5125–5130.
70. Tuschl, T. and Eckstein, F. (1993) *Proc. Natl. Acad. Sci. USA* **90**, 6991–6994.